Advances in Difference Equations
a SpringerOpen Journal

RESEARCH Open Access

A modified analytical approach with existence and uniqueness for fractional Cauchy reaction–diffusion equations

Sunil Kumar[1*], Amit Kumar[2], Syed Abbas[3], Maysaa Al Qurashi[4] and Dumitru Baleanu[5,6]

*Correspondence:
skiitbhu28@gmail.com;
skumar.math@nitjsr.ac.in
[1] Department of Mathematics, National Institute of Technology, Jamshedpur, India
Full list of author information is available at the end of the article

Abstract

This article mainly explores and applies a modified form of the analytical method, namely the homotopy analysis transform method (HATM) for solving time-fractional Cauchy reaction–diffusion equations (TFCRDEs). Then mainly we address the error norms L_2 and L_∞ for a convergence study of the proposed method. We also find existence, uniqueness and convergence in the analysis for TFCRDEs. The projected method is illustrated by solving some numerical examples. The obtained numerical solutions by the HATM method show that it is simple to employ. An excellent conformity obtained between the solution got by the HATM method and the various well-known results available in the current literature. Also the existence and uniqueness of the solution have been demonstrated.

Keywords: Homotopy analysis transform method; Fractional Cauchy reaction–diffusion equation; Mittag-Leffler function; Optimal value

1 Introduction

The beginning of fractional calculus is considered as 30 September 1695 when the derivative of arbitrary order was described by Leibniz [1]. After that many renowned mathematicians have studied the application of the fractional derivative and fractional differential equations (FDEs); some of them were Liouville, Grunwald, Letnikov and Riemann [2]. A lot of significant phenomena are well described by FDEs in electromagnetics, acoustics, viscoelasticity, electro chemistry and material science [3]. Moreover, some basic results associated to solving FDEs may be found in [4–7].

Cauchy reaction–diffusion equations (CRDEs) explain a large multiplicity of nonlinear systems in physics, chemistry, ecology, biology and engineering [8–12]. CRDEs are broadly used in application models for spatial effects in ecology. The different types of CRDEs in physics have been solved [13–15] by using a variety of kinds of analytical methods. In recent times, Yildirim [16] used a homotopy perturbation method to find the solutions of the CRDEs. In this paper, we consider the one-dimensional TFCRDEs as follows:

$$\frac{\partial^\lambda w(x,t)}{\partial t^\lambda} = D\frac{\partial^2 w(x,t)}{\partial x^2} + r(x,t)w(x,t), \quad 0 < \lambda \le 1, (x,t) \in \Omega \subset \mathbb{R}^2, \tag{1.1}$$

subject to the initial or boundary conditions

$$w(x,0) = g(x), \qquad w(0,t) = f_0(t), \qquad \frac{\partial w(0,t)}{\partial x} = f_1(t), \quad x,t \in \mathbb{R}, \tag{1.2}$$

where w is the concentration, r is the reaction parameter and $D > 0$ is the diffusion coefficient. The fractional derivative λ considered in this paper is in the sense of Caputo.

In this paper, we have applied HATM for solving linear and nonlinear TFCRDEs. The HATM method provides excellent agreement between two powerful methods, one is the most popular and useful homotopy analysis method (HAM) and the other one is the Laplace transform method. The HAM was first proposed and applied by Liao in [17] to solve lots of nonlinear problems. The HAM has been successfully applied by many researchers for solving linear and nonlinear partial differential equations [18, 19].

But presently, concentration of diverse researchers is on finding the solution behavior of different nonlinear equations by means of different methods jointed with Laplace transform, among them the variation iteration transform method [20] and the homotopy analysis transform method [21, 22]. The advantage of HATM over HAM is that it gives rapidly convergent series solution only by taking a small number of terms and hence HATM is very powerful and efficient in finding approximate solutions as well as analytical solutions of many fractional physical models. Moreover, the analytical method of using the Laplace transform and its inverse is shown in [23–25]. The other work related to this can be found in [26–34]. The plan of this article is to find approximate analytical solutions of TFCRDEs with the time derivative λ ($0 < \lambda \leq 1$).

2 Existence and uniqueness

In this section, we establish the existence and uniqueness of a solution of differential equation (1.1). We first present a few necessary definitions.

The Mittag-Leffler function is defined by

$$E_\lambda(t) = \sum_{k=0}^{\infty} \frac{t^{k\lambda}}{\Gamma(1+\lambda k)}. \tag{2.1}$$

The Riemann–Liouville fractional integral of order $\lambda > 0$ is defined by

$$I^\lambda f(t) = \frac{1}{\Gamma(\lambda)} \int_0^t (t-s)^{\lambda-1} f(s)\,ds, \tag{2.2}$$

the fractional derivative of the function f of order $\lambda > 0$ is defined by

$$D_t^\lambda f(t) = \frac{1}{\Gamma(n-\lambda)} \frac{d^n}{dt^n} \int_0^t (t-s)^{n-\lambda-1} f(s)\,ds, \tag{2.3}$$

where $\Gamma(\lambda)$ is the Gamma function.

The Laplace transform of the Riemann–Liouville fractional integral is defined as [1]

$$L\bigl[I^\lambda f(t)\bigr](s) = s^{-\lambda} \mathcal{F}(s). \tag{2.4}$$

The Caputo fractional derivative of the function f of order $\lambda > 0$ is defined by

$$D_t^{\lambda} f(t) = \frac{1}{\Gamma(n-\lambda)} \int_0^t t^{n-\lambda-1} \frac{d^n}{dt^n} f(t)\,dt. \tag{2.5}$$

The Laplace transform of the Caputo fractional derivative is defined as [1]

$$L\big[D_t^{\lambda} f(t)\big](s) = s^{\lambda}\mathcal{F}(s) - \sum_{k=0}^{n-1} s^{\lambda-k-1} f^k(0), \quad n-1 < \lambda \leq n, n \in \mathbb{N}. \tag{2.6}$$

Define an operator $A = D\frac{\partial^2}{\partial x^2}$, with $D(A) = \{v \in H_0^1(0,1) \cap H^2(0,1) : v'' \in L^2(0,1)\}$. The operator A is the infinitesimal generator of an analytic semigroup $\{T(t) : t \geq 0\}$ and is self-adjoint [35]. By introducing $v(t)x = w(x,t)$ and $\gamma(t)x = r(x,t)$, Eq. (1.1) can be written as

$$D_t^{\lambda} v = Av + \gamma(t)v. \tag{2.7}$$

By a mild solution v of the above problem we mean that

$$v(t) = v_0 + \frac{1}{\Gamma(\lambda)} A \int_0^t \frac{v(s)}{(t-s)^{1-\lambda}}\,ds + \frac{1}{\Gamma(\lambda)} \int_0^t \frac{\gamma(s)v(s)}{(t-s)^{1-\lambda}}\,ds, \tag{2.8}$$

provided $\int_0^t \frac{v(s)}{(t-s)^{1-\lambda}}\,ds \in \mathcal{D}$. The notation $\mathcal{D}$ is for the domain of the operator A equipped with the graph norm $\|v\|_{\mathcal{D}} = \|v\| + \|Av\|$. It is not difficult to check that $f(t,v) = \gamma(t)v$ satisfies the Lipschitz condition. For any $v_1, v_2 \in D(A)$, we have

$$\big\|f(t,v_1) - f(t,v_2)\big\| \leq \big|\gamma(t)\big| \|v_1 - v_2\| \leq \gamma^* \|v_1 - v_2\|,$$

where γ^* is the supremum of $\gamma(t)$. So we need $\gamma(t)$ to be continuous and bounded.

The spectrum of the operator A is discrete with eigenvalues $\mu_n = -n^2 D$, $n \in \mathbb{N}$, and the eigenfunctions are of the form $\psi_n(z) = (\frac{2}{\pi})^{\frac{1}{2}} \sin nz$. Moreover, $\{\psi_n : n \in \mathbb{N}\}$ is an orthonormal basis for X, and

$$T(t)v = \sum_{n=1}^{\infty} e^{-n^2 Dt} \langle v, \psi_n \rangle \psi_n, \quad v \in X, t > 0.$$

The above expression implies that $\{T(t), t \geq 0\}$ is a uniformly bounded compact semigroup and $R(\mu, A) = (\mu I - A)^{-1}$ is a compact operator for all $\mu \in \rho(A)$. The integral equation

$$v(t) = \frac{1}{\Gamma(\lambda)} \int_0^t \frac{Av(s)}{(t-s)^{1-\lambda}}\,ds, \quad t \geq 0,$$

has an associated resolvent operator $\{S_\lambda(t), t \geq 0\}$ on the space $X = L^2(0,1)$. The resolvent operator is given by

$$S_\lambda(t) = \frac{1}{2\pi i} \int_{\gamma_\theta} e^{\mu t} \big(\mu^{\lambda} - A\big)^{-1}\,d\mu, \quad t > 0,$$

and $S(0) = I$. We have the parameter θ with $\frac{\pi}{2} < \theta < \pi$ and the curve $\gamma_\theta = \{re^{i\theta} : r \geq 0\} \cup \{re^{-i\theta : r \geq 0}\}$.

Because $(\mu I - A)^{-1}$ is compact, from the above representation one can deduce that $\{S_\lambda(t) : t > 0\}$ is a compact operator.

Theorem 2.1 *Let $\gamma \in L^p([0,T] : \mathbb{R}^+)$ for $p = \frac{1}{\lambda}$. If $\frac{1}{\Gamma\lambda} \sup_{s\in[0,T]}(\int_0^s \frac{\gamma(t)}{(s-t)^{1-\alpha}}\,dt) < 1$, then the abstract Cauchy problem has a unique mild solution.*

The proof is similar to Theorem 2.1 of [36].

3 Fundamental scheme of HATM

The fundamental scheme of HATM is discussed through the following TFCRDEs:

$$\begin{aligned} &D_t^\lambda w(x,t) = DD_{xx}w(x,t) + r(x,t)w(x,t), \\ &0 < \lambda \le 1, \qquad (x,t) \in \Omega \subset R^2. \end{aligned} \tag{3.1}$$

By a new methodology discussed in [21], applied to Eq. (3.1), we get the mth-order deformation equation $w_m(x,t)$ and for $m \ge 1$, at Mth order, we have

$$w(x,t) = \sum_{m=0}^{M} w_m(x,t), \tag{3.2}$$

for $M \to \infty$, we get a precise approximation of the actual equation (3.1).

In this section, we study the convergence of HATM through the following theorem.

Theorem 3.1 *As long as the series solution*

$$w(x,t) = w_0(x,t) + \sum_{m=1}^{\infty} w_m(x,t) \tag{3.3}$$

converges, where $w_m(x,t)$ is governed by Eq. (3.1), it must be the exact solution of the TFCRDEs in (3.1).

Proof If the series (3.3) converges, we can write

$$T(x,t) = \sum_{m=0}^{\infty} w_m(x,t) \tag{3.4}$$

and

$$\lim_{m\to\infty} w_m(x,t) = 0. \tag{3.5}$$

We can verify that

$$\sum_{m=1}^{n} \big[w_m(x,s) - \xi_m w_{m-1}(x,s)\big] = \lim_{m\to\infty} w_m(x,s) = 0. \tag{3.6}$$

Taking the linear operator $\mathcal{L}$ on both sides in Eq. (3.6), we get

$$\sum_{m=1}^{\infty} \mathcal{L}\big[w_m(x,s) - \xi_m w_{m-1}(x,s)\big] = \mathcal{L}\left[\sum_{m=1}^{\infty} w_m(x,s) - \xi_m w_{m-1}(x,s)\right] = 0. \tag{3.7}$$

Along this line, we obtain

$$\sum_{m=1}^{\infty}\mathcal{L}\big[w_m(x,s)-\xi_m w_{m-1}(x,s)\big]=\hbar H(x,s)\sum_{m=1}^{\infty}R_m(\vec{w}_{m-1},x,s)=0, \tag{3.8}$$

since $\hbar \neq 0$ and $H(x,s)\neq 0$, from Eq. (3.8) we have

$$\sum_{m=1}^{\infty}R_m(\vec{w}_{m-1},x,s)=0, \tag{3.9}$$

$$\begin{aligned}\sum_{m=1}^{\infty}R_m(\vec{w}_{m-1},x,s)&=\sum_{m=1}^{\infty}\Bigg[s^{\lambda}L[w_{m-1}](s)-(1-\xi_m)\sum_{k=0}^{n-1}s^{\lambda-k-1}w_{m-1}^{k}(x,0)\\&\quad-L[DD_{xx}w_{m-1}+rw_{m-1}](s)\Bigg]\\&=s^{\lambda}L\Bigg[\sum_{m=1}^{\infty}w_{m-1}\Bigg](s)-\sum_{k=0}^{n-1}s^{\lambda-k-1}w_{m-1}^{k}(x,0)\\&\quad-L\Bigg[DD_{xx}\sum_{m=1}^{\infty}w_{m-1}+r\sum_{m=1}^{\infty}w_{m-1}\Bigg](s)\\&=s^{\lambda}L\big[T(x,t)\big](s)-\sum_{k=0}^{n-1}s^{\lambda-k-1}T^{k}(x,0)\\&\quad-L\big[DD_{xx}\big[T(x,t)\big]+r(x,t)\big[T(x,t)\big]\big](s)\\&=L\big[D_t^{\lambda}T(x,t)\big](s)-L\big[DD_{xx}T(x,t)+r(x,t)T(x,t)\big](s).\end{aligned}$$

Now from Eq. (3.9) we have

$$L\big[D_t^{\lambda}T(x,t)\big](s)-L\big[DD_{xx}T(x,t)+r(x,t)T(x,t)\big](s)=0. \tag{3.10}$$

By taking the inverse Laplace transform in Eq. (3.10), we get the exact solution $T(x,t)$. □

4 Function of HATM and mathematical results

Four examples of TFCRDEs are solved to exhibit the HATM method. In the whole article, MATHEMATICA 7 software package has been used for the figures' computational processes.

Example 1 For the constant value of $D=1$ and $r=-1$, Eq. (1.1) can be recast as the Kolmogorov–Piskunov (KP) equation [16] as follows:

$$\frac{\partial^{\lambda}w(x,t)}{\partial t^{\lambda}}=\frac{\partial^{2}w(x,t)}{\partial x^{2}}-w(x,t),\quad 0<\lambda\leq 1,(x,t)\in\Omega\subset\mathbb{R}^{2}, \tag{4.1}$$

subject to the initial or boundary conditions

$$\begin{aligned}&w(x,0)=e^{-x}+x=g(x),\qquad w(0,t)=1=f_0(t),\\&\frac{\partial w(0,t)}{\partial x}=E_{\lambda}\big(-t^{\lambda}\big)-1=f_1(t),\quad x,t\in\mathbb{R}.\end{aligned}$$

By a new methodology discussed in [21], applied to Eq. (4.1) we get the mth-order deformation equation for $w_m(x,t)$

$$w_m(x,t) = (\xi_m + \hbar)w_{m-1} - \hbar(1-\xi_m)\left(e^{-x}+x\right) - \hbar L^{-1}\left[s^{-\lambda}L[D_{xx}w_{m-1} - w_{m-1}](s)\right](t). \quad (4.2)$$

At last,

$$w(x,t) = w_0(x,t) + \sum_{m=0}^{\infty} w_m(x,t).$$

Next, the successive iterative values are

$$\begin{aligned}
w_1(x,t) &= \frac{\hbar x t^{\lambda}}{\Gamma(\lambda+1)},\\
w_2(x,t) &= \frac{\hbar(1+\hbar)xt^{\lambda}}{\Gamma(\lambda+1)} + \frac{\hbar^2 x t^{2\lambda}}{\Gamma(2\lambda+1)},\\
w_3(x,t) &= \frac{\hbar(1+\hbar)^2 xt^{\lambda}}{\Gamma(\lambda+1)} + \frac{2\hbar^2(1+\hbar) x t^{2\lambda}}{\Gamma(2\lambda+1)} + \frac{\hbar^3 x t^{3\lambda}}{\Gamma(3\lambda+1)},\\
w_4(x,t) &= \frac{\hbar(1+\hbar)^3 xt^{\lambda}}{\Gamma(\lambda+1)} + \frac{3h^2(1+\hbar)^2 x t^{2\lambda}}{\Gamma(2\lambda+1)} + \frac{3\hbar^3(1+\hbar) x t^{3\lambda}}{\Gamma(3\lambda+1)} + \frac{\hbar^4 x t^{4\lambda}}{\Gamma(4\lambda+1)} + \cdots.
\end{aligned}$$

In a similar fashion, the remaining terms of $w_m(x,t)$ for $m \geq 5$ can be entirely obtained.

Therefore, the solution of Eq. (4.1) is

$$w(x,t) = \sum_{k=0}^{\infty} w_k(x,t). \quad (4.3)$$

If we select $\hbar = -1$, then the solution is reduced to

$$\begin{aligned}
w(x,t) &= e^{-x} + x\left(1 + \frac{(-t^{\lambda})}{\Gamma(\lambda+1)} + \frac{(-t^{\lambda})^2}{\Gamma(2\lambda+1)} + \frac{(-t^{\lambda})^3}{\Gamma(3\lambda+1)} + \frac{(-t^{\lambda})^4}{\Gamma(4\lambda+1)} + \cdots\right)\\
&= e^{-x} + x\sum_{k=0}^{\infty} \frac{(-t^{\lambda})^k}{\Gamma(k\lambda+1)}\\
&= e^{-x} + xE_{\lambda}\left(-t^{\lambda}\right). \quad (4.4)
\end{aligned}$$

Again if we take the standard value of $\lambda = 1$, then the series solution is reduced to $e^{-x} + xe^{-t}$, this is an exact solution of standard CRDEs and hence the result is absolutely in conformity with the homotopy perturbation given by Yildirim [16] and the Adomian decomposition method by Lesnic [13].

Figure 1 demonstrates the comparisons of the exact solution and the approximate solutions with different Brownian motions. The picture of subfigures (a), (b), (c) and (d) for Fig. 1 shows that the approximate solution obtained by the current method and the exact solution are very much identical for the Cauchy problem with the constant term $D = 1$.

At the same time, in order to judge the significance and the correctness of the HATM method the absolute error curve is drawn in Fig. 2. It is to be noted that the approximate solution converges quickly towards the exact one.

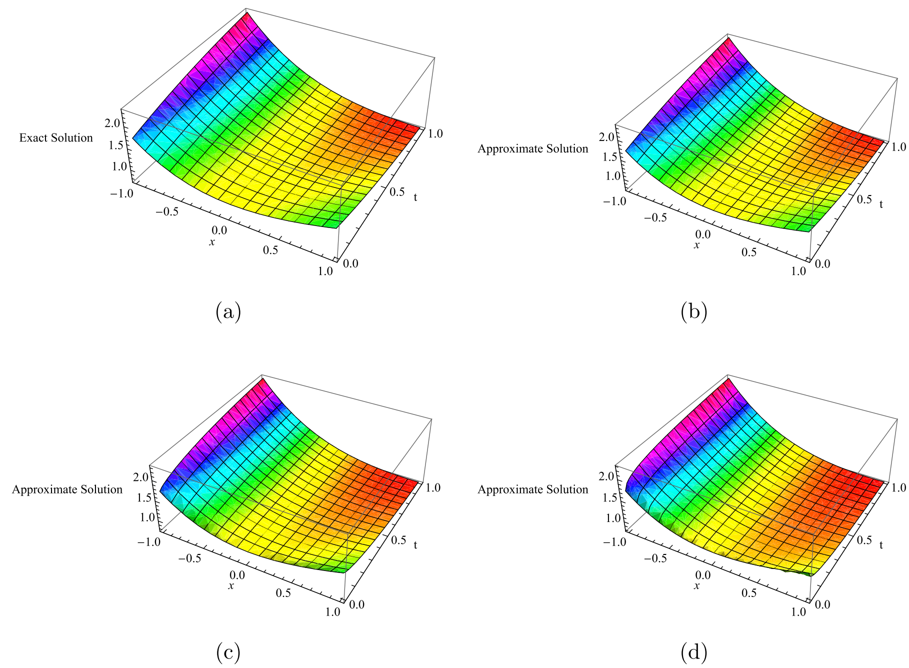

Figure 1 The surface graph of the exact solution $u(x,t)$ and the seventh-order approximate solution $u_7(x,t)$ of Eq. (4.1): (**a**) $u(x,t)$ when $\lambda = 1$, (**b**) $u_7(x,t)$ when $\lambda = 1$, (**c**) $u_7(x,t)$ when $\lambda = 0.75$, (**d**) $u_7(x,t)$ when $\lambda = 0.5$

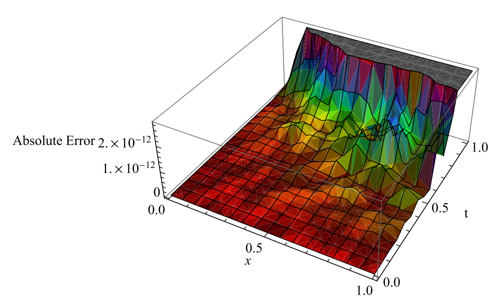

Figure 2 Plot of absolute error $E_7(w) = |w(x,t) - w_7(x,t)|$ using HATM when $\lambda = 1$

Figure 3 indicates the performance of the approximate solution for different fractional Brownian motions, $\lambda = 0.7, 0.8, 0.9$, and for standard motion i.e. at $\lambda = 1$.

Figure 4 reflects the $\hbar$ curve of Eq. (4.1). As pointed out by Liao [17], we can choose any values of $\hbar$, where $\hbar \in (\hbar_1, \hbar_2)$ and $\hbar_1 \approx -1.80$, $\hbar_2 \approx -0.2$. In the particular case if $\hbar = -1$ the speed of convergence is most advantageous.

In order to convergence study of the proposed method we present the absolute errors in Table 1, simultaneously the error norms L_2 and L_∞ are presented in Table 2.

At the mth order of approximation, also we can define the exact square residual error for equation, where

$$\Delta_m = \int_0^1 \int_0^1 \left(N\left[\sum_{i=0}^{m} w_i(x,t) \right] \right)^2 dx\, dt,$$

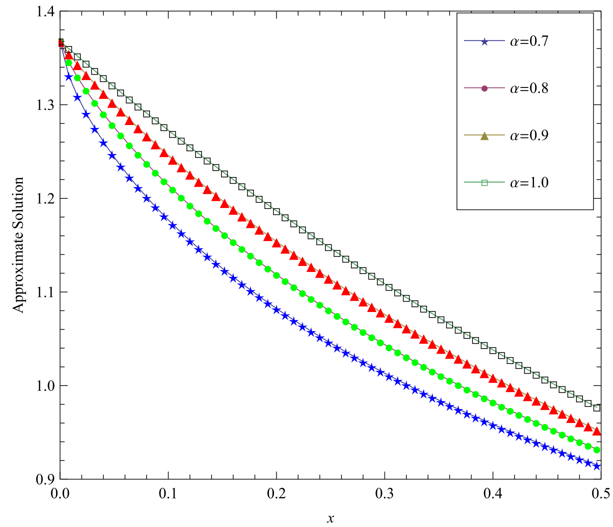

Figure 3 Plot of $u(x,t)$ verses x time for different values of λ at $t = 1$ and $\hbar = -1$

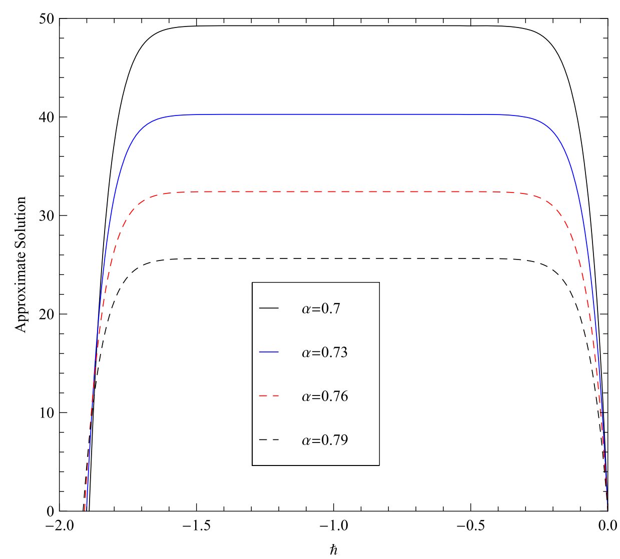

Figure 4 Plot of $\hbar$ curve for different values of λ at $x = 0.5$ and $t = 0.01$

where

$$N\left[w(x,t)\right] = \frac{d^{\lambda}w(x,t)}{dt^{\alpha}} - \frac{d^2w(x,t)}{dx^2} + w(x,t).$$

In order to make things computationally easy we also introduced here the so-called averaged residual error defined by

$$E_m = \frac{1}{25}\sum_{j=1}^{5}\sum_{k=1}^{5}\left(N\left[\sum_{i=0}^{m}u_i\left(\frac{j}{10},\frac{k}{10}\right)\right]\right)^2.$$

Table 1 E_7 in the solution of TFCRDEs using HATM for $\lambda = 1$

(x,t)	Exact solution	Approximation solution	$\lvert u_{\text{exact}} - u_{\text{MHATM}}\rvert$
(0.1, 0.1)	0.9953211598	0.9953211598	9.99201×10^{-15}
(0.1, 0.2)	0.9867104933	0.9867104933	2.95319×10^{-14}
(0.1, 0.3)	0.9789192401	0.9789192401	1.68754×10^{-14}
(0.2, 0.1)	0.9996982366	0.9996982366	2.27596×10^{-14}
(0.2, 0.2)	0.9824769036	0.9824769036	6.20615×10^{-14}
(0.2, 0.3)	0.9668943972	0.9668943972	8.32667×10^{-15}
(0.3, 0.1)	1.0122694460	1.0122694460	2.55351×10^{-14}
(0.3, 0.2)	0.9864374466	0.9864374466	4.32987×10^{-14}
(0.3, 0.3)	0.9630636868	0.9630636868	4.39648×10^{-14}

Table 2 L_2 and L_∞ error norms for TFCRDEs by HATM for $\lambda = 1$

x	L_2 error norm	L_∞ error norm
0.1	1.87998×10^{-14}	1.68754×10^{-14}
0.2	3.10492×10^{-14}	8.32667×10^{-15}
0.3	3.18634×10^{-14}	4.39648×10^{-14}

Table 3 Optimal value of $\hbar$ for $\lambda = 1$

Order of approximation	Optimal value of $\hbar$	Value of E_m
2	−0.826476	8.9631×10^{-1}
4	−0.939232	8.90047×10^{-1}
6	−0.964903	8.8997×10^{-1}

Table 4 Optimal value of $\hbar$ for $\lambda = 0.9$

Order of approximation	Optimal value of $\hbar$	Value of E_m
2	−0.79381	8.84405×10^{-1}
4	−0.918672	8.73643×10^{-1}
6	−0.950037	8.73404×10^{-1}

The optimal value of $\hbar$ can be found by solving nonlinear algebraic equation $\frac{dE_m}{d\hbar} = 0$ [37]. The numerical results are elaborated in Tables 3 and 4.

It is clear from Tables 3 and 4 that the optimal value of $\hbar$ are −0.826476, −0.939232, −0.964903 and −0.79381, −0.918672, −0.950037, respectively, in the case of different orders of approximations.

Example 2 We take the following TFCRDEs [16] for $D = 1$ and $r(x,t) = -1 - 4x^2$:

$$\frac{\partial^\lambda w(x,t)}{\partial t^\lambda} = \frac{\partial^2 w(x,t)}{\partial x^2} - \left(1 + 4x^2\right) w(x,t), \quad 0 < \lambda \le 1, (x,t) \in \Omega \subset \mathbb{R}^2, \tag{4.5}$$

subject to the initial or boundary conditions

$$w(x,0) = e^{x^2} = g(x), \qquad w(0,t) = E_\lambda\left(t^\lambda\right) = f_0(t), \qquad \frac{\partial w(0,t)}{\partial x} = 0 = f_1(t), \quad x,t \in \mathbb{R}.$$

Now similar to Example 1, the mth-order deformation equation (4.5) is

$$\begin{aligned} w_m(x,t) &= (\xi_m + \hbar)w_{m-1} - \hbar(1-\xi_m)e^{x^2} - \hbar L^{-1}\bigl[s^{-\lambda}L\bigl[D_{xx}w_{m-1} \\ &\quad - \bigl(4x^2+1\bigr)w_{m-1}\bigr](s)\bigr](t). \end{aligned} \tag{4.6}$$

At last, we get

$$w(x,t) = w_0(x,t) + \sum_{m=0}^{\infty} w_m(x,t).$$

By taking $w_0(x,t) = w(x,0) = e^{x^2}$ and the system (4.6), we get the subsequent values as follows:

$$\begin{aligned} w_1(x,t) &= -\frac{\hbar e^{x^2} t^{\lambda}}{\Gamma(\lambda+1)}, \\ w_2(x,t) &= -\frac{\hbar(1+\hbar)e^{x^2} t^{\lambda}}{\Gamma(\lambda+1)} + \frac{\hbar^2 e^{x^2} t^{2\lambda}}{\Gamma(2\lambda+1)}, \\ w_3(x,t) &= -\frac{\hbar(1+\hbar)^2 e^{x^2} t^{\lambda}}{\Gamma(\lambda+1)} + \frac{2\hbar^2(1+\hbar)e^{x^2} t^{2\lambda}}{\Gamma(2\lambda+1)} - \frac{\hbar^3 e^{x^2} t^{3\lambda}}{\Gamma(3\lambda+1)}, \\ w_4(x,t) &= -\frac{\hbar(1+\hbar)^3 e^{x^2} t^{\lambda}}{\Gamma(\lambda+1)} + \frac{3\hbar^2(1+\hbar)^2 e^{x^2} t^{2\lambda}}{\Gamma(2\lambda+1)} - \frac{3\hbar^3(1+\hbar)e^{x^2} t^{3\lambda}}{\Gamma(3\lambda+1)} + \frac{\hbar^4 e^{x^2} t^{4\lambda}}{\Gamma(4\lambda+1)} + \cdots. \end{aligned}$$

The solution of Eq. (4.5) for $\hbar = -1$ is given as

$$\begin{aligned} w(x,t) &= e^{x^2}\left(1 + \frac{t^{\lambda}}{\Gamma(\lambda+1)} + \frac{t^{2\lambda}}{\Gamma(2\lambda+1)} + \frac{t^{3\lambda}}{\Gamma(3\lambda+1)} + \frac{t^{4\lambda}}{\Gamma(4\lambda+1)} + \cdots\right) \\ &= e^{x^2}\sum_{k=0}^{\infty}\frac{t^{k\lambda}}{\Gamma(k\lambda+1)} \\ &= e^{x^2}E_{\lambda}\bigl(t^{\lambda}\bigr). \end{aligned} \tag{4.7}$$

Next for the standard value of $\lambda = 1$, the above series solution reduced to $e^{-x} + xe^{-t}$, this is an exact solution of standard CRDEs and hence the result is absolutely conformity with that the homotopy perturbation given by Yildirim [16] and the Adomian decomposition method by Lesnic [13].

Figure 5 shows the comparison between the exact and the approximate solution for Example 2 obtained by HATM for different values of λ.

Again, the convergence of the above method for Eq. (4.5) is shown by drawing the absolute error curve.

Figure 6 represents the absolute error between exact and obtained solution.

Figure 7 reveals the performance of the estimated solution $w(x,t)$ for Example 2.

In Fig. 8 the $\hbar$ curve for Eq. (4.5) is shown. It is clear from Fig. 8 that the perfect range of $\hbar$ is from -1.60 to -0.3.

Table 5 lists the absolute error $E_7 = |w(x,t) - w_7(x,t)|$ obtained for different values of x and t by using the seventh-order approximate solution. Again, to show the validity and exactness of the proposed method the error norms L_2 and L_∞ are presented in Table 6.

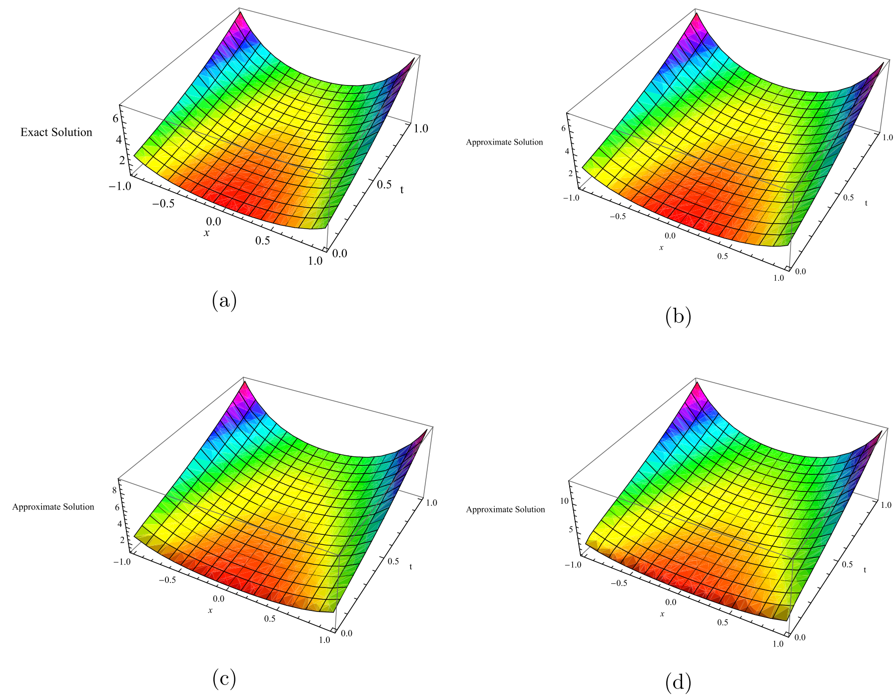

Figure 5 The surface graph of the exact solution $u(x,t)$ and the seventh-order approximate solution $u_7(x,t)$ of Eq. (4.5): (**a**) $u(x,t)$ when $\lambda = 1$, (**b**) $u_7(x,t)$ when $\lambda = 1$, (**c**) $u_7(x,t)$ when $\lambda = 0.75$, (**d**) $u_7(x,t)$ when $\lambda = 0.5$

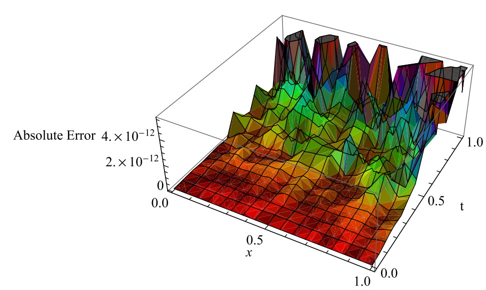

Figure 6 Plot of absolute error $E_7(w) = |w(x,t) - w_7(x,t)|$ using HATM when $\lambda = 1$

Example 3 We consider the following TFCRDEs [14] for $D = 1$ and $r(x,t) = -1 + \cos x - \sin^2 x$:

$$\frac{\partial^\lambda w(x,t)}{\partial t^\lambda} = \frac{\partial^2 w(x,t)}{\partial x^2} - \left(-1 + \cos x - \sin^2 x\right) w(x,t), \quad 0 < \lambda \le 1, (x,t) \in \Omega \subset \mathbb{R}^2, \tag{4.8}$$

subject to the initial or boundary conditions

$$w(x,0) = \frac{1}{10} e^{\cos x - 11} = g(x), \qquad w(0,t) = \frac{1}{10} e^{-10} E_\lambda\left(t^{-\alpha}\right) = f_0(t),$$
$$\frac{\partial w(0,t)}{\partial x} = 0 = f_1(t).$$

The exact solution $w(x,t) = \frac{1}{10} e^{\cos x - t - 11}$ for $\lambda = 1$.

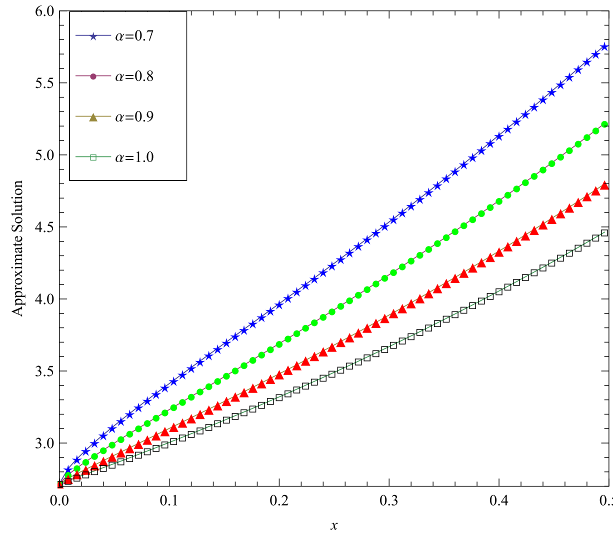

Figure 7 Plot of $u(x,t)$ verses x time for different values of λ at $t = 1$ and $\hbar = -1$

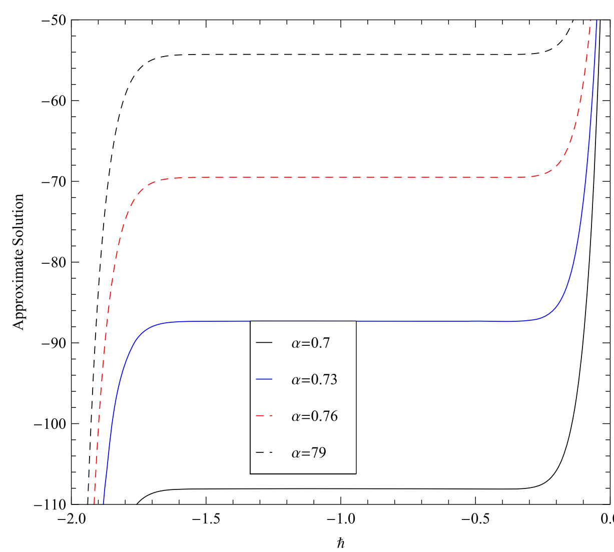

Figure 8 Plot of $\hbar$ curve for different values of λ at $x = 0.5$ and $t = 0.01$

By using the aforementioned techniques, in this case the solution of the mth-order deformation equations is as follows:

$$\begin{aligned} w_m(x,t) = {}& (\xi_m + \hbar)w_{m-1} - \hbar(1-\xi_m)e^{x^2} - \hbar L^{-1}\big[s^{-\lambda}L\big[D_{xx}w_{m-1} \\ & - \big(-1+\cos x - \sin^2 x\big)w_{m-1}\big](s)\big](t). \end{aligned} \tag{4.9}$$

By taking $w_0(x,t) = w(x,0) = \frac{1}{10}e^{\cos x - 10}$ and the system (4.6), we get the subsequent values as follows:

$$w_1(x,t) = \frac{\hbar e^{-11+\cos x}t^{\lambda}}{10\Gamma(\lambda+1)},$$

Table 5 E_7 in the solution of TFCRDEs by HATM for $\lambda = 1$

(x,t)	Exact solution	Approximation solution	$\lvert u_{\text{exact}} - u_{\text{MHATM}} \rvert$
(0.1, 0.1)	1.1162780704	1.1162780704	4.62963×10^{-12}
(0.1, 0.2)	1.2336780599	1.2336780599	7.89258×10^{-12}
(0.1, 0.3)	1.3634251141	1.3634251141	6.866828×10^{-12}
(0.2, 0.1)	1.1502737988	1.1502737988	2.49134×10^{-13}
(0.2, 0.2)	1.2712491580	1.2712491580	3.77920×10^{-13}
(0.2, 0.3)	1.4049475905	1.4049475905	4.90874×10^{-12}
(0.3, 0.1)	1.0122694460	1.0122694460	7.84484×10^{-13}
(0.3, 0.2)	1.3364274882	1.3364274882	6.75904×10^{-13}
(0.3, 0.3)	1.4769807938	1.4769807938	3.81584×10^{-12}

Table 6 The error norm in the solution of TFCRDEs by HATM for $\lambda = 1$

x	L_2 error norm	L_∞ error norm
0.1	6.4635×10^{-12}	6.866828×10^{-12}
0.2	1.84526×10^{-12}	4.90874×10^{-12}
0.3	1.75874×10^{-12}	3.81584×10^{-12}

$$w_2(x,t) = \frac{\hbar(1+\hbar)e^{-11+\cos x}t^{\lambda}}{10\Gamma(\lambda+1)} + \frac{\hbar^2 e^{-11+\cos x}t^{2\lambda}}{10\Gamma(2\lambda+1)},$$
$$w_3(x,t) = \frac{\hbar(1+\hbar)^2e^{-11+\cos x}t^{\lambda}}{10\Gamma(\lambda+1)} + \frac{\hbar^2(1+\hbar)e^{-11+\cos x}t^{2\lambda}}{5\Gamma(2\lambda+1)} + \frac{\hbar^3 e^{-11+\cos x}t^{3\lambda}}{10\Gamma(3\lambda+1)}.$$

If we select $\hbar = -1$, then

$$\begin{aligned} w(x,t) &= \frac{1}{10}e^{\cos x-11} - \frac{e^{\cos x-11}t^{\lambda}}{10\Gamma(\lambda+1)} + \frac{e^{\cos x-11}t^{2\lambda}}{10\Gamma(2\lambda+1)} + \frac{e^{\cos x-11}t^{3\lambda}}{11\Gamma(3\lambda+1)} + \cdots \\ &= \frac{1}{10}e^{\cos x-11}\left[1 - \frac{t^{\lambda}}{\Gamma(\lambda+1)} + \frac{t^{2\lambda}}{\Gamma(2\lambda+1)} + \frac{t^{3\lambda}}{\Gamma(3\lambda+1)} + \cdots\right] \\ &= \frac{1}{10}e^{\cos x-11}\sum_{k=0}^{\infty}\frac{(-t)^k}{\Gamma(k\lambda+1)} \\ &= \frac{1}{10}e^{\cos x-11}E_{\lambda}\left(-t^{\alpha}\right). \end{aligned} \tag{4.10}$$

For $\lambda = 1$, this series is reduced to the closed form $\frac{1}{10}e^{\cos x-t-11}$, which is an exact solution of the classical CRDEs and hence the result is absolutely in conformity with the variation iteration method given by Dehghan [14].

Figure 9 shows the assessment among the exact and estimated solution. To ensure the exactness of the HATM method the absolute error curve is given in Fig. 10. Again, Fig. 11 shows the performance of the $u_7(x,t)$ for diverse term of λ.

Figure 12 shows the $\hbar$ curve. Here we can choose any values of $\hbar$, where $\hbar \in (\hbar_1, \hbar_2)$ and $\hbar_1 \approx -1.70$, $\hbar_2 \approx -0.5$.

Example 4 Here we have taken the following TFCRDEs [38]:

$$\frac{\partial^{\lambda} w(x,t)}{\partial t^{\lambda}} = \frac{\partial}{\partial x}\left(w\frac{\partial w}{\partial x}\right) + w - w^2, \quad 0 < \lambda \le 1, x, t \ge 0, \tag{4.11}$$

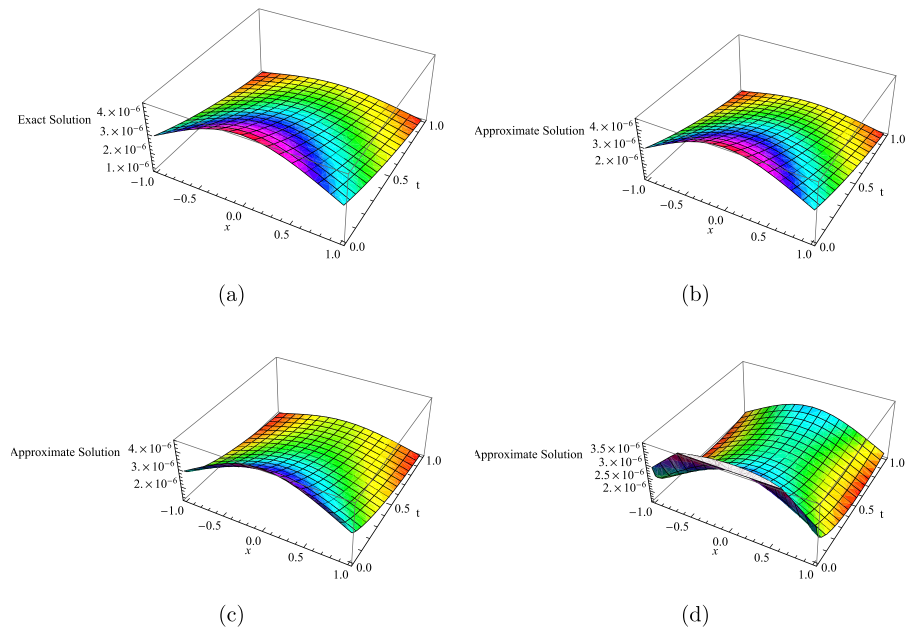

Figure 9 The surface graph of the exact solution $u(x,t)$ and the seventh-order approximate solution $u_7(x,t)$ of Eq. (4.8): (**a**) $u(x,t)$ when $\lambda = 1$, (**b**) $u_7(x,t)$ when $\lambda = 1$, (**c**) $u_7(x,t)$ when $\lambda = 0.75$, (**d**) $u_7(x,t)$ when $\lambda = 0.5$

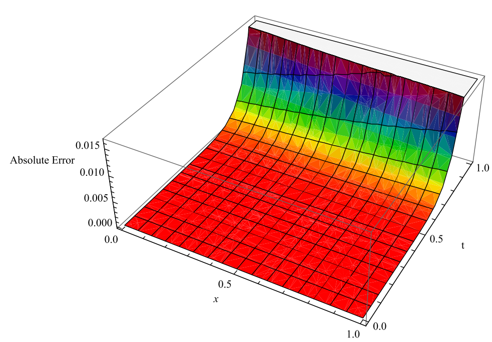

Figure 10 Plot of absolute error $E_7(w) = |w(x,t) - w_7(x,t)|$ using HATM when $\lambda = 1$

subject to the initial or boundary conditions

$$w(x,0) = 1 - e^{\frac{-x}{\sqrt{2}}} = g(x), \qquad w(0,t) = 1 - E_\lambda\left(-t^{\frac{\lambda}{2}}\right) = f_0(t),$$
$$\frac{\partial w(0,t)}{\partial x} = \frac{1}{\sqrt{2}} E_\lambda\left(-t^{\frac{\lambda}{2}}\right) = f_1(t).$$

The exact solution $w(x,t) = 1 - e^{\frac{-x}{\sqrt{2}} - \frac{t}{2}}$ for $\lambda = 1$.

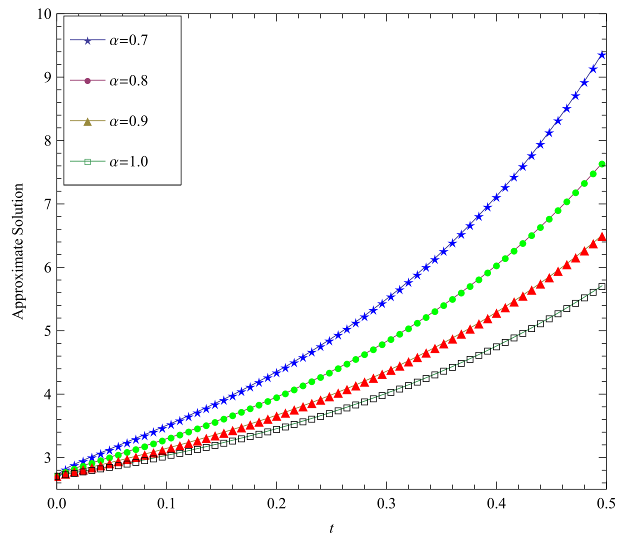

Figure 11 Plot of $u(x,t)$ verses x time for different values of λ at $t = 1$ and $\hbar = -1$

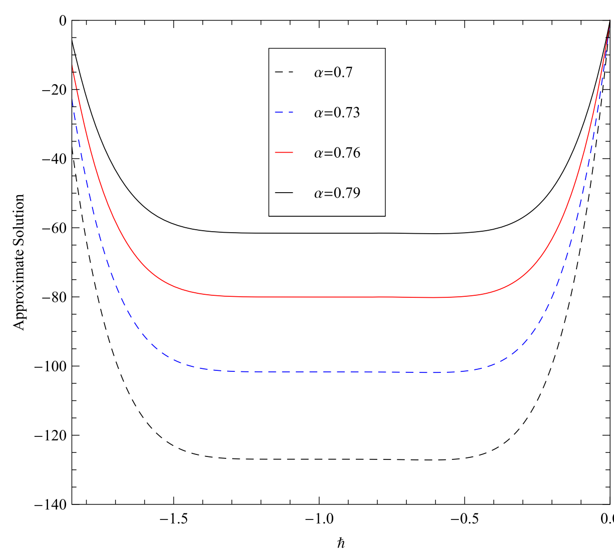

Figure 12 Plot of $\hbar$ curve for different values of λ at $x = 0.5$ and $t = 0.01$

By using the aforementioned techniques, in this case the solution of the mth-order deformation equations is as follows:

$$w_m(x,t) = (\xi_m + \hbar)w_{m-1} - \hbar(1-\xi_m)\left(1 - e^{\frac{-x}{\sqrt{2}}}\right) - \hbar L^{-1}\left[s^{-\lambda} L\left[\sum_{k=0}^{\infty}\left(w_{m-1-k}(w_k)_x\right)_x + w_{m-1} - \sum_{k=0}^{\infty} w_{m-1-k}(w_k)\right](s)\right](t). \tag{4.12}$$

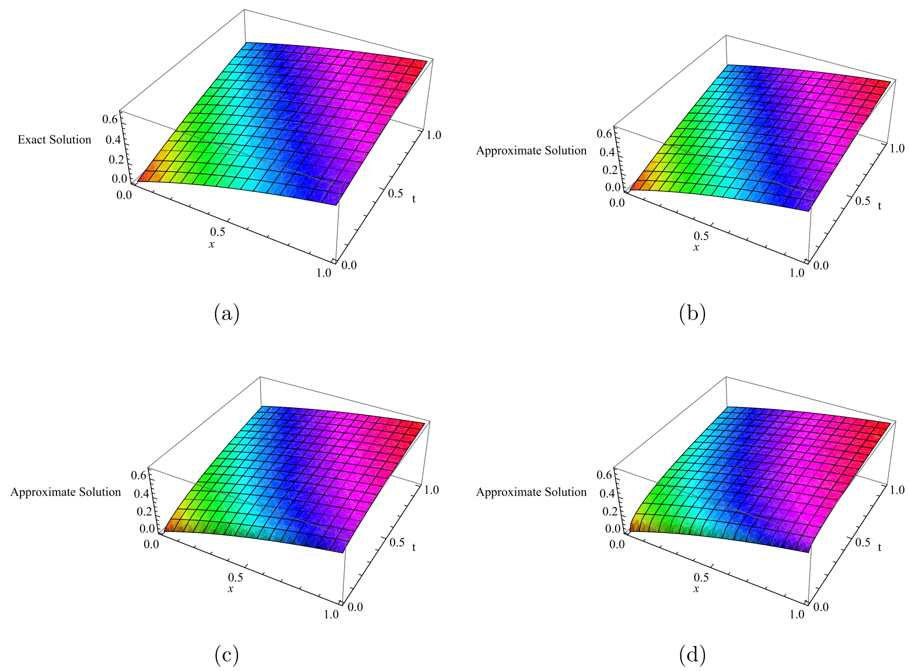

Figure 13 The surface graph of the exact solution $u(x,t)$ and the seventh-order approximate solution $u_7(x,t)$ of Eq. (4.11): (**a**) $u(x,t)$ when $\lambda = 1$, (**b**) $u_7(x,t)$ when $\lambda = 1$, (**c**) $u_7(x,t)$ when $\lambda = 0.75$, (**d**) $u_7(x,t)$ when $\lambda = 0.5$

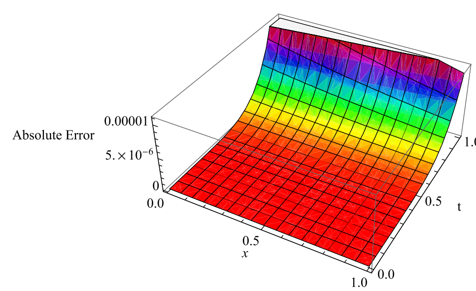

Figure 14 Plot of absolute error $E_7(w) = |w(x,t) - w_7(x,t)|$ using HATM when $\lambda = 1$

By taking $w_0(x,t) = w(x,0) = 1 - e^{\frac{-x}{\sqrt{2}}}$ and the system (4.6), we get the subsequent values as follows:

$$w_1(x,t) = \frac{-\hbar e^{\frac{-x}{\sqrt{2}}} t^{\lambda}}{2\Gamma(\lambda+1)},$$

$$w_2(x,t) = \frac{-\hbar(1+\hbar) e^{\frac{-x}{\sqrt{2}}} t^{\lambda}}{2\Gamma(\lambda+1)} - \frac{\hbar^2 e^{\frac{-x}{\sqrt{2}}} t^{\lambda}}{4\Gamma(2\lambda+1)},$$

$$w_3(x,t) = \frac{-\hbar(1+\hbar)^2 e^{\frac{-x}{\sqrt{2}}} t^{\lambda}}{2\Gamma(\lambda+1)} - \frac{\hbar^2(1+\hbar) e^{\frac{-x}{\sqrt{2}}} t^{2\lambda}}{2\Gamma(2\lambda+1)} - \frac{\hbar^3 e^{\frac{-x}{\sqrt{2}}} t^{3\lambda}}{8\Gamma(3\lambda+1)}.$$

Figure 13 shows the comparison between the exact and approximate solution obtained by HATM method. The absolute error curve is presented in Fig. 14.

Acknowledgements
All authors would like to express their sincere thanks to the respected editors for their time and comments as regards the review process. The first author Dr. Sunil Kumar would like to acknowledge the financial support received from the National Board for Higher Mathematics, Department of Atomic Energy, Government of India (Approval No. 2/48(20)/2016/NBHM(R.P.)/R and D II/1014).

Funding
Not applicable.

Competing interests
The authors declare that they have no competing interests.

Authors' contributions
All authors contributed equally and significantly in writing this paper and typed, read, and approved the final manuscript.

Author details
[1]Department of Mathematics, National Institute of Technology, Jamshedpur, India. [2]Department of Mathematics, Balarampur College Purulia, Balarampur, India. [3]School of Basic Sciences, Indian Institute of Technology Mandi, Mandi, India. [4]Department of Mathematics, King Saud Uniersity, Riyadh, Saudi Arabia. [5]Department of Mathematics, Cankya University, Ankara, Turkey. [6]Institute of Space Science, Magurele-Bucharest, Romania.

Publisher's Note

Springer Nature remains neutral with regard to jurisdictional claims in published maps and institutional affiliations.

Received: 19 February 2019 Accepted: 29 December 2019 Published online: 15 January 2020

References

1. Oldham, K.B., Spanier, J.: The Fractional Calculus: Theory and Applications of Differentiation and Integration to Arbitrary Order. Academic Press, San Diego (1994)
2. Miller, K.S., Ross, B.: An Introduction to the Fractional Calculus and Fractional Differential Equations. Wiley, New York (2003)
3. Podlubny, I.: Fractional Differential Equations. Academic Press, London (1999)
4. Diethelm, K., Ford, N.J.: Analysis of fractional differential equations. J. Math. Anal. Appl. **265**, 229–248 (2002)
5. Diethelm, K.: An algorithms for the numerical solutions of differential equations of fractional order. Electron. Trans. Numer. Anal. **5**, 1–6 (1997)
6. Abbas, S.: Existence of solutions to fractional order ordinary and delay differential equations and applications. Electron. J. Differ. Equ. **2011**, Article ID 9 (2011)
7. Abbas, S., Banerjee, M., Momani, S.: Dynamical analysis of fractional-order modified logistic model. Comput. Math. Appl. **62**, 1098–1104 (2011)
8. Britton, N.F.: Reaction–Diffusion Equations and Their Applications to Biology. Academic Press, New York (1998)
9. Cantrell, R.S., Cosner, C.: Spatial Ecology via Reaction–Diffusion Equations. Wiley Series in Mathematical and Computational Biology. Wiley, New York (2003)
10. Grindrod, P.: The Theory and Applications of Reaction–Diffusion Equations, 2nd edn. Oxford Applied Mathematics and Computing Science Series. Oxford University Press, New York (1996)
11. Rothe, F.: Global Solutions of Reaction–Diffusion Systems. Lecture Notes in Mathematics. Springer, Berlin (1984)
12. Smoller, J.: Shock Waves and Reaction–Diffusion Equations, 2nd edn. Grundlehren der Mathematischen Wissenschaften (Fundamental Principles of Mathematical Sciences). Springer, New York (1994)
13. Lesnic, D.: The decomposition method for Cauchy reaction–diffusion problems. Appl. Math. Lett. **20**, 412–418 (2007)
14. Dehghan, M., Shakeri, F.: Application of He's variational iteration method for solving the Cauchy reaction–diffusion problem. J. Comput. Appl. Math. **214**, 435–446 (2008)
15. Baeumer, B., Kovacs, M., Meerschaert, M.M.: Numerical solutions for fractional reaction–diffusion equations. Comput. Math. Appl. **55**, 2212–2226 (2008)
16. Yildirim, A.: Application of He's homotopy perturbation method for solving the Cauchy reaction–diffusion problem. Comput. Math. Appl. **57**, 612–618 (2009)
17. Liao, S.J.: The proposed homotopy analysis techniques for the solution of nonlinear problems. Ph.D. dissertation, Shanghai Jiao Tong University, Shanghai, China (1992)
18. Vishal, K., Kumar, S., Das, S.: Application of homotopy analysis method for fractional swift Hohenberg equation—revisited. Appl. Math. Model. **36**, 3630–3637 (2012)
19. Abbasbandy, S., Shirzadi, A.: The series solution of problems in the calculus of variations via the homotopy analysis method. Z. Naturforsch. A **64**, 30–36 (2009)
20. Arife, A.S., Yildirim, A.: New modified variational iteration transform method for solving eighth-order boundary value problems in one step. World Appl. Sci. J. **13**(10), 2186–2190 (2012)
21. Kumara, S., Kumar, A., Odibat, Z.: A nonlinear fractional model to describe the population dynamics of two interacting species. Math. Methods Appl. Sci. **40**(11), 4134–4148 (2017)
22. Kumar, S., Kumar, A., Argyros, I.K.: A new analysis for the Keller–Segel model of fractional order. Numer. Algorithms **75**(1), 213–228 (2017)
23. Khader, M., Kumar, S., Abbasbandy, S.: Fractional homotopy analysis transforms method for solving a fractional heat-like physical model. Walailak J. Sci. Technol. **13**(5), 337–353 (2016)
24. Kumar, S.: A new analytical modelling for fractional telegraph equation via Laplace transform. Appl. Math. Model. **38**(13), 3154–3163 (2014)

25. Víctor, M.D., Gómez-Aguilar, J.F., Huitzilin, Y.M., Baleanu, D., Escobar Jiménez, R., Victor, O.P.: Laplace homotopy analysis method for solving linear partial differential equations using a fractional derivative with and without kernel singular. Adv. Differ. Equ. **2016**, Article ID 164 (2016)
26. Wu, G.C., Zeng, D.Q., Baleanu, D.: Fractional impulsive differential equations: exact solutions, integral equations and short memory case. Fract. Calc. Appl. Anal. **22**, 180–192 (2019)
27. Wu, G.C., Deng, Z.G., Baleanu, D., Zeng, D.Q.: New variable-order fractional chaotic systems for fast image encryption. Chaos Solitons Fractals **29**, Article ID 083103 (2019)
28. Doungmo Goufoa, E.F., Kumar, S., Mugisha, S.B.: Similarities in a fifth-order evolution equation with and with no singular kernel. Chaos Solitons Fractals **130**, Article ID 109467 (2020)
29. Odibat, Z., Kumar, S.: A robust computational algorithm of homotopy asymptotic method for solving systems of fractional differential equation. J. Comput. Nonlinear Dyn. **14**(8), Article ID 081004 (2019)
30. El-Ajou, A., Oqielat, M.N., Al-Zhour, Z., Kumar, S., Momani, S.: Solitary solutions for time-fractional nonlinear dispersive PDEs in the sense of conformable fractional derivative. Chaos **29**, Article ID 093102 (2019)
31. Kumar, S., Kumar, A., Momani, S., Aldhaifalla, M., Nisar, K.S.: Numerical solutions of nonlinear fractional model arising in the appearance of the strip patterns in two-dimensional systems. Adv. Differ. Equ. **2019**, Article ID 413 (2019)
32. Sharma, B., Kumar, S., Cattani, C., Baleanu, D.: Nonlinear dynamics of Cattaneo–Christov heat flux model for third-grade power-law fluid. J. Comput. Nonlinear Dyn. **15**(1), Article ID 011009 (2019)
33. Singh, A., Das, S., Ong, S.H., Jafari, H.: Numerical solution of nonlinear reaction–advection–diffusion equation. J. Comput. Nonlinear Dyn. **14**(4), Article ID 041003 (2019)
34. Tripathi, N.K., Das, S., Ong, S.H., Jafari, H., Qurashi, M.M.A.: Solution of time-fractional Cahn–Hilliard equation with reaction term using homotopy analysis method. Adv. Mech. Eng. **9**(12), 1–7 (2017)
35. Pazy, A.: Semigroups of Linear Operators and Applications to Partial Differential Equations. Applied Math. Sci. Springer, New York (1983)
36. Hernandez, E., Regan, D.O., Balachandran, K.: Existence results for abstract fractional differential equations with nonlocal conditions via resolvent operators. Indag. Math. **24**, 68–82 (2013)
37. Liao, S.J.: An optimal homotopy-analysis approach for strongly nonlinear differential equations. Commun. Nonlinear Sci. Numer. Simul. **15**, 2003–2016 (2010)
38. Nourazar, S.S., Nazari-Golshan, A., Nourazar, M.: On the closed form solutions of linear and nonlinear Cauchy reaction–diffusion equations using the hybrid of Fourier transform and variational iteration method. Phys. Int. **2**(1), 8–20 (2011)